

Liquid Phase Deposition of Transition Metal Ferrite Thin Films: Synthesis and Magnetic Properties

Gabriel Caruntu and Charles J. O'Connor[†]

Advanced Materials Research Institute, Chemistry Department, University of New Orleans, New Orleans, LA, USA
(Received October 19, 2006; Accepted October 31, 2006)

ABSTRACT

We report on the synthesis of highly uniform, single phase zinc and cobalt thin films prepared by the Liquid Phase Deposition (LPD) method. X-Ray diffraction, TGA and EDX measurements support the assumption that the as deposited films are constituted by a mixture of crystallized FeOOH and amorphous M(OH)₂ (M=Co, Zn) which is converted upon heat treatment in air at 600°C into the corresponding zinc ferrites. The films with adjustable chemical compositions are identified with a crystal structure as spinel-type and present a spherical or rod-like microstructure, depending on the both the nature and concentration of the divalent transition metal ions. Zinc ferrite thin films present a superparamagnetic behavior above blocking temperatures which decrease with increasing the Zn content and are ferromagnetic at 5 K with coercivities ranging between 797.8 and 948.5 Oe, whereas the cobalt ferrite films are ferromagnetic at room temperature with magnetic characteristics strongly dependent on the chemical composition.

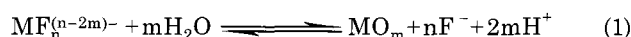
Key words: Ferrite, Thin film, Synthesis, Magnetic properties

1. Introduction

Transition metal ferrites MFe₂O₄ are one of the most important family of technological materials, due to their remarkable properties which find use in many applications in the next generation electronics, catalysis and magnetic information storage. Although ferrites are traditionally prepared in bulk, the miniaturization of magnetic and electronic devices has demanded advanced materials with new forms and shapes, such as nanoparticles or thin films. Ferrite thin films can typically be deposited onto various substrates by various synthetic techniques which can be categorized as physical and chemical methods, respectively. Physical methods include molecular beam epitaxy,^{1,2)} magnetron sputtering^{3,4)} or Pulse Laser Deposition (PLD),^{5,6)} whereas chemical processes include Chemical Vapor Deposition (CVD),^{7,8)} electrodeposition,⁹⁾ electroless deposition,¹⁰⁾ hydrothermal,¹¹⁾ spin spraying,^{12,13)} dip coating¹⁴⁾ and spin coating of sol-gel reagents.^{15,16)}

Although these methods allow for the preparation of ferrite films tailorable to particular applications, in most cases they present several critical shortcomings, *i.e.*, the need of expensive and sophisticated equipment to create vacuum or a low pressure atmosphere, the thickness of the films cannot be controlled accurately during deposition, the line-of-sight deposition has limitations and films are often difficult

to be deposited onto surfaces with large areas or complex morphologies. The development of new synthetic strategies for the selective deposition of multicomponent oxide films is important for the future of microelectronic circuitry. In the last years, a novel chemical method, called Liquid Phase Deposition (LPD) was proposed by Nagayama and coworkers¹⁷⁾ for the synthesis of metal oxide thin films. It consists of the direct precipitation of homogenous metal oxide films via the controlled hydrolysis of the corresponding solutions of transition metal-fluoro complexes in presence of aluminum or boric acid (1). Control over the hydrolysis process is necessary in order to prevent spontaneous bulk precipitation of the solution.



Boric acid or aluminum acts as a scavenger for the fluoride ions by forming a stable complex [BF₄]⁻ ion, which causes the equilibrium reaction (1) to proceed to the right side with formation of the metal oxide.



Initially developed for SiO₂¹⁸⁾ and TiO₂¹⁹⁾ films, the Liquid Phase Deposition (LPD) method has rapidly been extended to other transition metal oxides (V, Cr, Mn, Fe, Co, Ni, In, Nb, Cu, Zn),²⁰⁻²⁴⁾ FeOOH and α-Fe₂O₃,²⁵⁾ and Au-dispersed TiO₂ films,²⁶⁾ respectively. Because the main process involved is a homogenous nucleation from aqueous solutions, liquid phase deposition harbors great promise for the fabrication of multicomponent metal oxide films. However, extension of the liquid phase deposition to other oxide systems seemed to be limited, mainly due to the optimization of

[†]Corresponding author: C. J. O'Connor
E-mail: coconnor@uno.edu
Tel: +1-504-280-6840 Fax: +1-504-280-3185

reaction conditions so that both transition metal can be rendered hydrolysable simultaneously, which often results in absence of the chemical reaction.

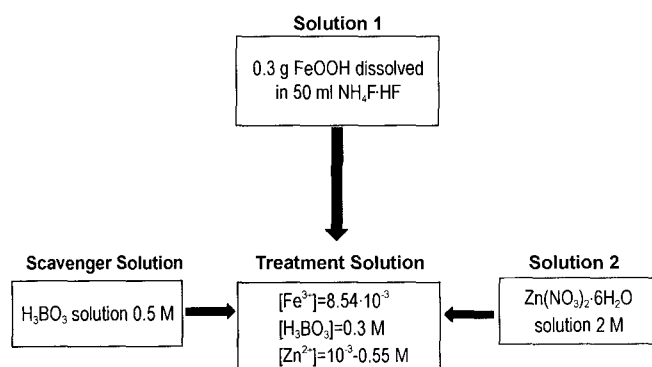
Consequently, considerably less is known on using the liquid phase deposition method to synthesize single phase multicomponent oxide films. Gao and coworkers deposited polycrystalline perovskite-type ABO_3 ($A = \text{Sr, Ba}$) thin films with a columnar morphology,²⁷ whereas Deki and coworkers reported the formation of iron-nickel binary oxide films.²⁸ However, the prepared nickel ferrite samples show very poor crystallinity upon annealing at high temperature as well as the mechanism of formation of ferrites is not very well elucidated. To our knowledge, there are no other reports on the deposition of ferrite films by this soft solution process. The present investigation aims at the extension of the liquid phase deposition method to the preparation of nanocrystalline ferrite thin films. We report here our initial, successful attempts in developing the liquid phase deposition method for the synthesis of cobalt and zinc ferrite films with variable chemical composition and tunable magnetic properties.

2. Experimental Procedure

2.1. Preparation of Ferrite Films by Chemical Deposition

The experiments were performed in open atmosphere using a magnetic hotplate with an external temperature controller. Source chemicals were reagent grade purity and used as received from Alfa Aesar. Deionized water (18 M Ω) was obtained from a Barnstead Nanopure water purification system. Scheme 1 shows the details of the synthetic strategy used to deposit zinc ferrite films by the liquid deposition method. Prior to deposition, the substrates were degreased by washing repeatedly with acetone and then sonicated in MilliQ water. The parent solution was obtained by dissolving 0.25 g of $\text{FeO}(\text{OH})$ in 50 ml of 1 M $\text{NH}_4\text{F} \cdot \text{HF}$ aqueous solution. FeOOH was precipitated from an aqueous solution of $\text{Fe}(\text{NO}_3)_3 \cdot 7\text{H}_2\text{O}$ upon addition of a diluted solution of ammonia.

The precipitate was then filtered, washed several times with distilled water and allowed to dry at room temperature



Scheme 1. Synthetic strategy used to deposit zinc ferrite films by liquid phase deposition (LPD) method.

in open air for several days. Then, a separate aqueous solution of M^{2+} ($\text{M} = \text{Co, Zn}$) with a concentration of 2 M was prepared by dissolving the corresponding amount of transition metal nitrate in distilled water.

Ferrite thin films were deposited on non-alkali glass plates (Corning no. 7059) substrates and p-type {111} single crystal Si wafers, respectively. Three separate aqueous solutions of iron hydroxide, $\text{M}(\text{NO}_3)_2$ ($\text{M} = \text{Co, Ni}$) and boric acid ($c = 0.5$ M) were mixed in different proportions to obtain a final solution with fixed concentrations of iron and H_3BO_3 , whereas the concentration of the M^{2+} was varied in the range $10^{-3} - 5.5 \times 10^{-1}$ M. Substrates were suspended vertically and soaked in the reaction solution at different temperatures ranging between 25°C and 65°C for different periods of time, typically ranging between 3 and 24 h. After being removed from the reaction solution, the films were carefully rinsed with distilled water, then sonicated and dried in open atmosphere. To ensure complete crystallization of the ferrite films, samples were subjected to a heat treatment in open air at 600°C followed by a natural cooling to room atmosphere.

2.2. Characterization of the Ferrite Films

Surface morphology and microstructure of the films was studied by using a JEOL-JSM 5410 scanning electron microscope, whereas their thicknesses were measured by a surface profile measuring system Dektak-IIA. Identification of the crystalline phases, crystallite size and the phase purity of the films were examined by X-ray diffraction using a Philips X'Pert System equipped with a curved graphite single-crystal monochromator (CuK_α radiation). Patterns were recorded in a step scanning mode in the 20-95° 2 θ range with a step of 0.02° and a counting time of 10s. The metal contents of the deposited ferrite films were determined by Inductive Coupled Plasma (ICP) spectroscopy, using a Varian FT220s flame absorption spectrometer. The correlation coefficient used to calibrate the instrument was 0.999147 and the calibration error did not exceed 5%. The corresponding solutions were prepared by dissolving the films in 18% HCl and then diluting them to the required concentrations.

Examination of the thermal behavior of the as grown films was performed using a TA Instrument TGA 2950. Approximately 5 mg of powdered sample were heated under flowing air (flow rate 25 ml/min) from room temperature to 600°C in an alumina crucible. Infrared spectra were collected with a Nicolet Magna 750 FTIR instrument. Samples were prepared by mixing the ferrite powders obtained by scratching the films with KBr and then pelletized. Then, spectra were recorded over the range of $\lambda = 4000$ to 500 cm^{-1} with a resolution of 5 cm^{-1} . Magnetic properties were investigated with a Quantum Design MPMS-5S SQUID magnetometer.

3. Results and Discussion

A low temperature, single step deposition of solutions of

transition metal salts in $\text{NH}_4\text{F} \cdot \text{HF}$ leads to highly uniform, well adherent zinc ferrite films with thickness which can be easily controlled by varying the deposition time. On the course of the deposition process, the initial colorless treatment solution turns slowly to a brownish colloidal suspension which becomes progressively clear and colorless as the chemical deposition of the films is achieved. The pH of the solution slightly increased from 4–5 to 6, which is presumably ascribed to the formation of basic transition-metal oxides/oxyhydroxides as a result of the simultaneous hydrolysis of the corresponding salts. Additionally, an amorphous brown fine powder was detected at the bottom of the reaction vessel as well as a thin light brown film on its walls. This clearly indicates that films form through the attachment of primarily fine particles of transition metal oxides/hydroxides originally precipitated in the bulk solution as a result of the hydrolysis of the transition-metal oxy-fluoro-complexes. In Fig. 1(a) is represented the evolution of the Zn/Fe ratio of the deposited ferrite films obtained from ICP measurements with increasing of the zinc concentration in the treatment solution.

The elemental analysis performed by EDX has shown that the films are fluorine free and chemically homogenous through the whole surface. Additionally, the composition of films deposited after 2, 4, 6, 12, and 24 h did not reveal major differences in the Zn/Fe ratio, which indicates that the chemical composition does not vary during the deposition process. Fig. 1(a) reveals the existence of two growth regimes, that is for initial concentrations of $[\text{Zn}^{2+}]$ ranging between 10^{-3} M and 10^{-2} M the curve shows an logarithmic character, whereas when $[\text{Zn}^{2+}] > 0.1$ M it becomes linear. This trend is consistent with that observed for the variation of the Zn/Fe ratio with the Zn content of the treatment solution (Fig. 1(c)) suggesting that the composition of the film is solely dictated by the Zn/Fe ratio of the treatment solution.

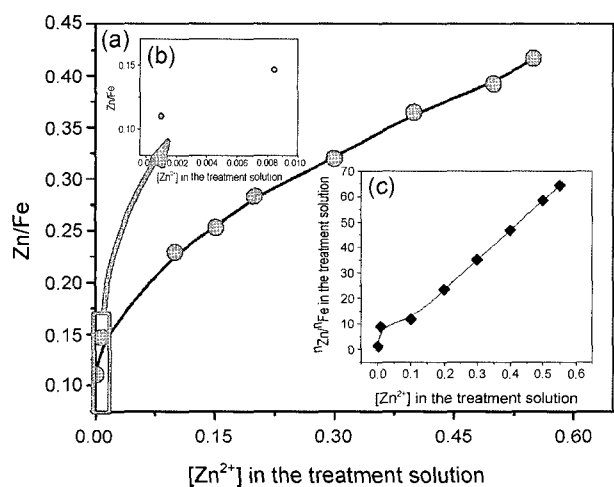


Fig. 1. (a) Variation of the Zn/Fe ratio of the film with the Zn^{2+} concentration of the reaction solution, (b) close-up of Fig. 1(a) in the concentration range of 10^{-3} – 10^{-2} M, and (c) variation of the Zn/Fe ratio in the treatment solution with the concentration of Zn^{2+} ion.

Assuming a stoichiometric Fe/O ratio in the prepared ferrites, the corresponding film composition as determined by ICP spectroscopy is indicated in Table 1. The error in measuring the elemental composition of the films was less than 5%. As expected, the Zn content of the deposited films increases progressively with increasing the Zn^{2+} concentration in the treatment solution. Ferrite films with highly tunable chemical composition can be obtained by liquid phase deposition by simply controlling the volumes of transition metal salts in the treatment solution. This is important since mastery of the chemical composition of ferrite films has proven to be critical for further technological applications.

In addition to the concentration of the initial solutions, temperature was found to play an important role on the kinetics of ferrite deposition. For a given deposition time, the increase of the reaction temperature accelerates the chemical deposition which, in turn results in thicker films. However, when reaction was performed at room temperature no precipitate was observed even after 3 days. As shown in Fig. 2, the film thickness varies roughly linearly with the deposition time and was found to range typically between 50 and 960 nm for a deposition time of 2–24 h, depending on the temperature.

It is important to note that the composition of the as deposited films is very sensitive to the reaction conditions. When ordinary distilled water is used to prepare the reaction solutions, akaganeite $\text{FeO}(\text{OH}, \text{Cl})$ (JCPDS 13-157) was deposited instead of β -lepidocrocite $\text{FeO}(\text{OH})$ (JCPDS 08-0098) which is obtained when using MilliQ water. In Fig. 4 are illustrated the X-ray diffraction patterns of the ferrite films before and after the heat treatment, respectively.

Regardless of the nature of the divalent metal, the X-ray diffraction patterns of the as-deposited ferrite films exhibit peaks which can be indexed as crystalline $\text{FeO}(\text{OH})$ (Fig. 1(a)). Since the divalent metals (Co,Zn) were not detected by

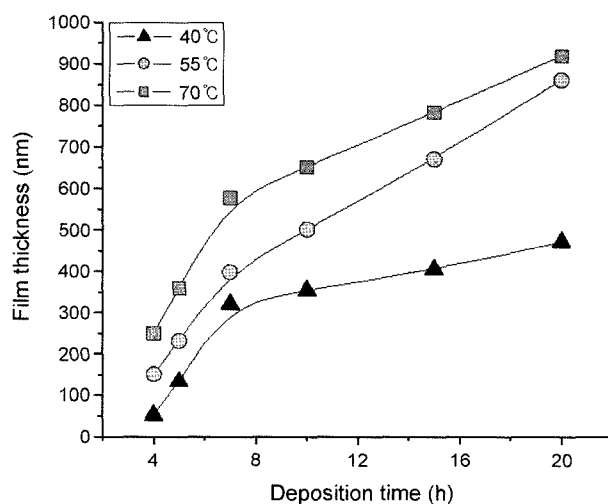


Fig. 2. Dependence of the film thicknesses on the deposition time at different reaction temperatures.

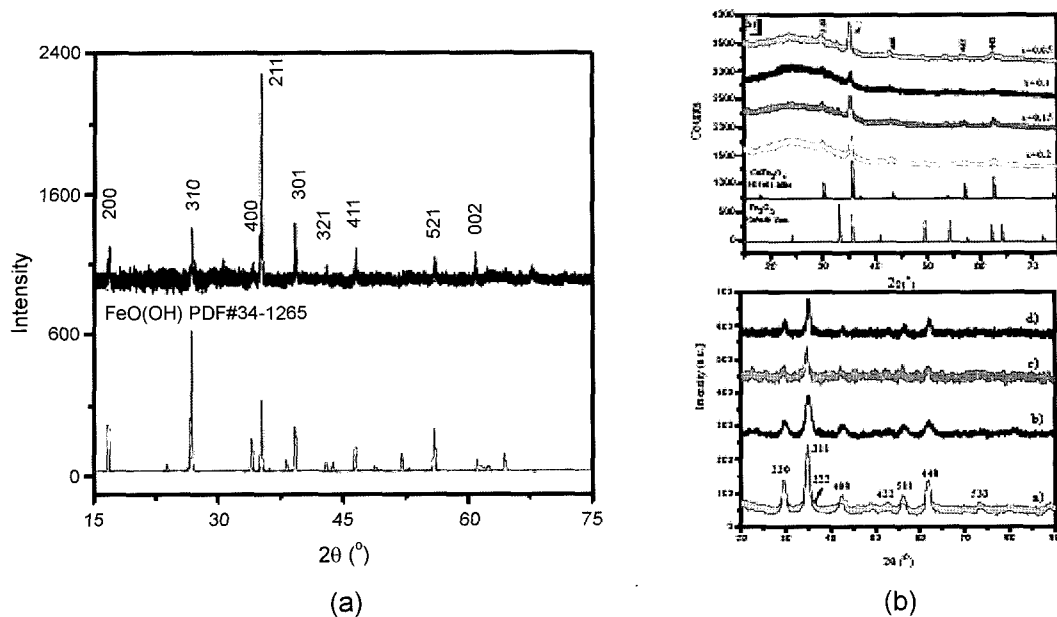


Fig. 3. Typical X-ray diffraction patterns of the as prepared (a) and annealed Co (b) and Zn ferrite (c) films with different chemical compositions.

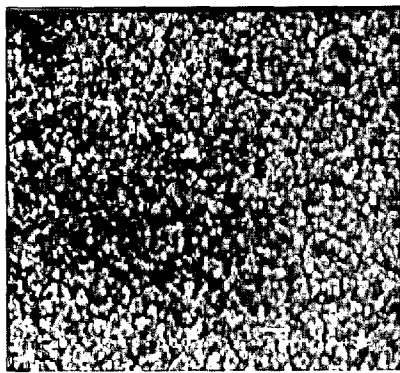


Fig. 4. Top-down SEM micrographs of a 200 nm $\text{Co}_{0.2}\text{Fe}_{2.8}\text{O}_4$ film deposited onto a Corning glass after heat treatment at 600°C.

X-ray diffraction, but they are found in solution by ICP measurements, we hypothesize that they are present in the as-prepared films as amorphous $\text{M}(\text{OH})_2$ phases. As shown in Fig. 4(b) and (c), the annealed films exhibit similar patterns although the samples correspond to different concentrations of the metals in the starting solution. Additionally, the relative intensities of the peaks do not exhibit preferred orientation growth. In all cases, a broad pattern originating from the substrate dominated the experimental diffraction peaks. Background subtraction was performed by using the PowderX suite of programs.²⁹⁾ All the experimental reflections are assigned to those of the standard polycrystalline MFe_2O_4 ($\text{M}=\text{Co},\text{Zn}$) which clearly indicates the formation of a spinel-type structure. However, in the case of the Co-ferrite films, for $x=0.05$ and 0.15 , a small reflection is observed at $\approx 33^\circ$ in 2θ and can be ascribed to a $\alpha\text{-Fe}_2\text{O}_3$ secondary phase. The small $\alpha\text{-Fe}_2\text{O}_3$ impurity is presumably associ-

ated to the presence of a slight excess of iron in the corresponding treatment solutions and further confirms that the liquid-phase deposition method allows the fine tuning of the chemical composition of the ferrite films via a rigorous control of the metal ratio in the treatment solutions. For the film with the chemical composition of $\text{Co}_{0.1}\text{Fe}_{2.9}\text{O}_4$, the XRD peaks were indexed into a spinel-type cubic lattice with a refined cell parameter of $a=8.38(4)$ Å, value which is in a good agreement with that reported for the bulk CoFe_2O_4 material ($a=8.392$ Å), whereas the refined lattice parameter of the film with the chemical composition of $\text{Zn}_{0.84}\text{Fe}_{2.16}\text{O}_4$ is $a=8.449(3)$ Å, which is consistent with that of the standard bulk zinc ferrite ($a=8.4411$ Å).³⁰⁾ In this latter case, the crystallite size of the film was further determined from the modified Scherrer's formula³¹⁾ gives a mean crystallite size of 20 nm.

In Fig. 4 is illustrated a typical SEM micrograph of the $\text{Co}_{0.2}\text{Fe}_{2.8}\text{O}_4$ film after annealing at 600°C. The film is composed by spherical-shaped densely packed particles with a mean diameter of 150 nm.

While the morphology of the Co-ferrite films is independent on the concentration of the Co^{2+} ions in the reaction solution, in the case of Zn ferrite films the shape of the consisting particles varies from spherical to rod-like with increasing the zinc content (Fig. 5). Typically, the films are composed by spherical-shaped densely packed particles with a mean diameter of 200 nm, value which is in a good agreement to those previously reported by Deki and coworkers for $\beta\text{-FeO}(\text{OH})/\alpha\text{-Fe}_2\text{O}_3$ films obtained by the same synthetic approach.²⁵⁾

Highly homogeneous films with a columnar architecture are observed in all cases, except the reaction solution whose zinc concentration is 0.1 M where the particles forming the

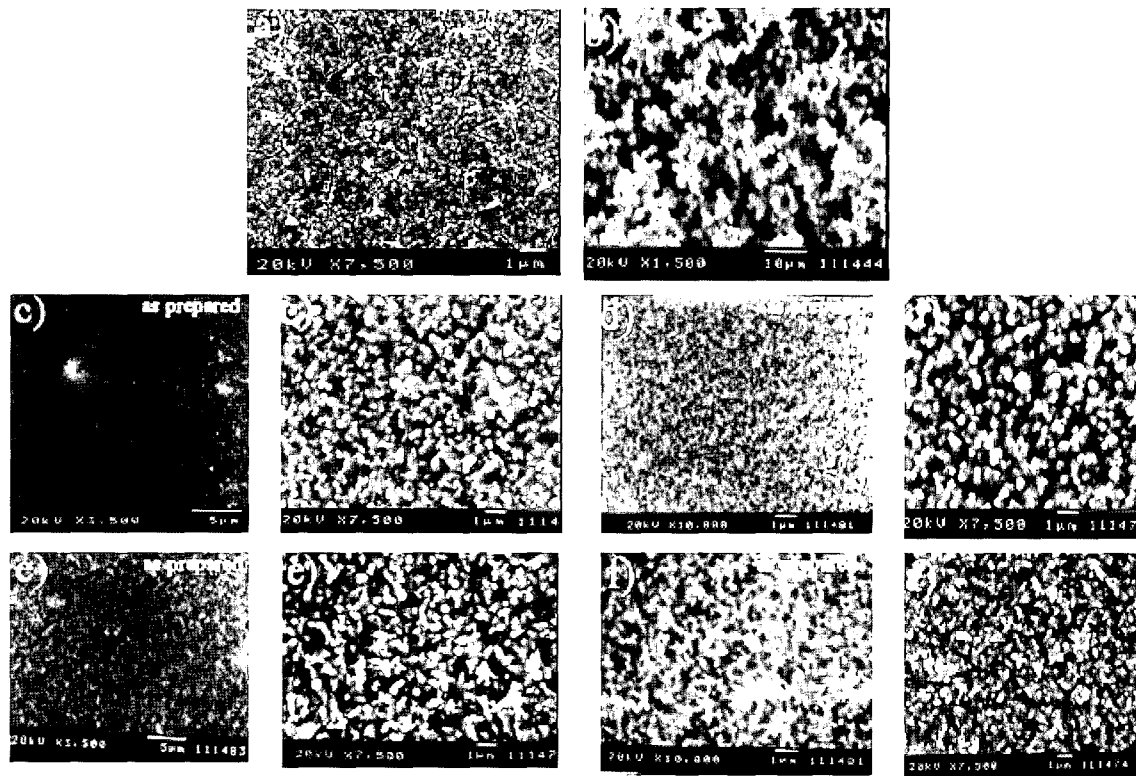


Fig. 5. Top-down SEM micrographs of zinc ferrite films deposited onto a Corning glass substrate from starting solutions with different Zn^{2+} concentrations (a=0 M, b=0.1 M, c=0.2 M, d=0.3 M, e=0.4 M, and f=0.5 M). Fig. 5(a) and (b) show annealed films, whereas Fig. 5(c)-(f) show both the as deposited film the annealed films, respectively.

film retain the spherical shape similar to that observed in the case of the $\alpha\text{-Fe}_2\text{O}_3$ film. Although there is not clear evidence about the role played by Zn^{2+} ions on the morphology of the resulted films, experimental data show that the increase of the Zn^{2+} concentration is accompanied by a change of the morphology of the deposited films from spherical to rod-like type. Additionally, as in most cases reported in liquid-phase deposition-based processing of thin films, it seems that deposition proceeds through heterogeneous nucleation of primary particles in solution followed by surface-directed growth.^{32,33} In the other cases, films are constructed by large arrays of well defined rod-like particles perpendicularly grown to the substrate surface whose diameter ranges between 250–320 nm. The diameter of the nanorods doesn't vary noticeably with the concentration of divalent ions in the reaction solution, but was found to be influenced by the reaction time. The ferrite films were characterized by using standard Zero-Field-Cooling (ZFC) and Field-Cooling (FC) procedures. The temperature dependence of the magnetization was measured between 5 K and 300 K under an external static magnetic field of 100 Oe, as shown in Fig. 6. Coercivity was measured at low temperature for each sample, whereas at room temperature no hysteresis was detected.

Zinc ferrite films exhibit a superparamagnetic behavior with blocking temperatures depending on the zinc content, whereas the cobalt ferrite films are ferromagnetic at room

temperature. The magnetic behavior observed experimentally is typical for all the zinc ferrite samples investigated, with small variations of the values of the saturation magnetization and coercivity.

The blocking temperature and saturation magnetization roughly decreases with increasing the zinc composition of the samples. Below the critical temperature T_c , the samples exhibit a ferrimagnetic behavior, which is related to the cationic disorder of the two sublattices (denoted by A for tetrahedral and B for octahedral, respectively) of the spinel structure. The coercivity is found to increase with increasing the Zn content of the films, whereas the values of the magnetization saturation fall within the range reported in literature for zinc ferrites.³⁴ However, the saturation magnetization is much lower than is the case of ZnFe_2O_4 films obtained by rf sputtering, whose magnetization at 5 K was reported to be 90 emu/g for a cation distribution given by the formula $(\text{Zn}_{0.4}\text{Fe}_{0.6})^{\text{tet}}(\text{Zn}_{0.6}\text{Fe}_{1.4})^{\text{oct}}\text{O}_4$.³⁵ Such a lower value of the saturation magnetization originates from a much smaller fraction of Fe^{2+} ions distributed over the tetrahedral sites which gives rise to a net magnetic moment of the tetrahedral sublattice and, in turn, enhances the A-B interactions at the expense of the B-B ones.

As for the Co-ferrite films, the squariness was found to vary only slightly with the composition, having an average value of $\text{SQ}=0.64$, whereas the saturation magnetization calculated by interpolating the high field values of the mag-

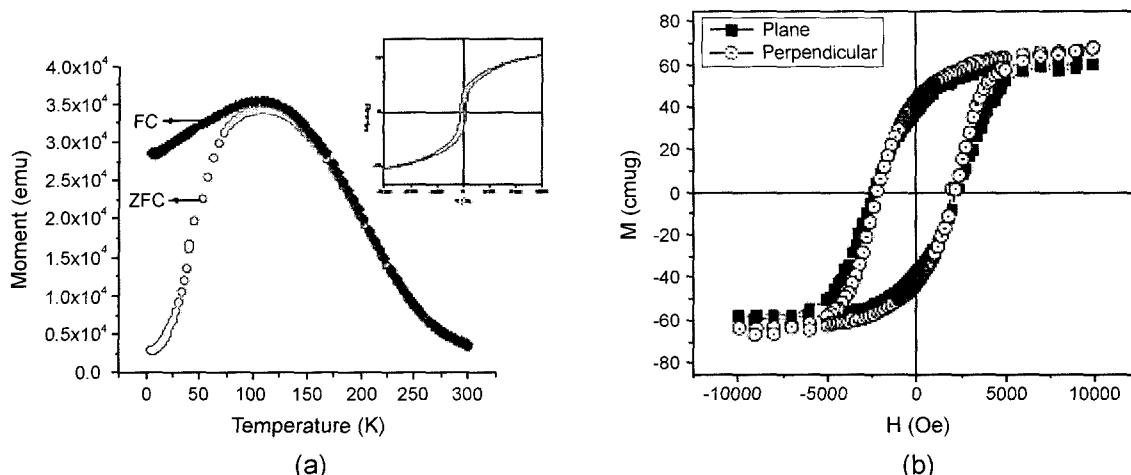


Fig. 6. ZFC and FC curves of $\text{Zn}_{0.73}\text{Fe}_{2.27}\text{O}_4$ film (a) and room temperature hysteresis loops of $\text{Co}_x\text{Fe}_{3-x}\text{O}_4$ ($x=0.05$) (b). The inset represents the hysteresis loop of the zinc ferrite film recorded at 5 K.

netization was found to decrease with increasing of the cobalt content of the films. Furthermore, for $x < 0.1$ the values of the saturation magnetization M_s are close to the bulk value which indicates that the Co^{2+} ions occupy mainly the octahedral sites and confirms the high quality of these films.

4. Conclusions

The liquid phase deposition offers a simple, feasible, non toxic and easy scalable aqueous low temperature route to the synthesis of single phase ferrite thin films. Highly homogeneous films have a chemical composition which can be easily controlled through tailoring the concentration of metal ions in the reaction solution. The resulting ferrite films present a complex morphology, being constructed by particles with spherical or rod-like shapes, which seem to be influenced to certain extent by the concentration of zinc ions in the reaction solution. Magnetic properties of the prepared Zn ferrite films show a superparamagnetic behavior with blocking temperatures ranging from 88 to 107 K, whereas the cobalt ferrite films are ferromagnetic at room temperature. The extension of the liquid phase deposition method to the preparation of other important transition metal ferrite films is currently pursued and will be reported elsewhere.

Acknowledgment

The authors gratefully acknowledge DARPA for funding through Grant No. MDA 972-97-1-0003.

REFERENCES

1. T. Tsurumi, T. Suzuki, M. Yamaze, and M. Daimon, "Fabrication of Barium Titanate/Strontium Titanate Artificial Superlattice by Atomic Layer Epitaxy," *Jpn. J. Appl. Phys.*, **33** 5192 (1994).
2. I. Wane, F. Cosset, A. Bessaudou, A. Celerier, C. Girault, J. L. Decossas, and J. C. Vareille, "Hard Ferrite Films Prepared by Electron Beam Evaporation for Microwave Applications," *Biannual Meeting of the Federation of European Materials Societies*, **9** 54-61 (1999).
3. M. Tachiki, M. Noda, K. Yamada, and T. Kobayashi, "SrTiO₃ Films Epitaxially Grown by Eclipse Pulsed Laser Deposition and their Electrical Characterization," *J. Appl. Phys.*, **83** 5351 (1998).
4. H. Y. Zhang, B. X. Gu, H. R. Zhai, and M. Lu, "Magnetic and Magneto-Optical Properties of Sputtered $\text{Co}_{0.8}\text{Fe}_{2.2}\text{O}_4$ Films with Perfect [111] Orientation," *Phys. Stat. Sol.*, **143** 399 (1994).
5. D. Ravinder, K. V. Kumar, and A. V. R. Reddy, "Preparation and Magnetic Properties of Ni-Zn Ferrite Thin Films," *Mater. Lett.*, **57** 4162 (2003).
6. P. C. Dorsey, P. Lubitz, D. B. Chrisey, and J. S. Horwitz, "CoFe₂O₄ Thin Films Grown on (100) MgO Substrates Using Pulsed Laser Deposition," *J. Appl. Phys.*, **79** [8] 6338 (1996).
7. P. A. Lane, P. J. Wright, M. J. Crosbie, A. D. Pitt, C. L. Reeves, B. Cockayne, A. C. Jones, and T. J. Leedham, "Liquid Injection Metal Organic Chemical Vapour Deposition of Nickel Zinc Ferrite Thin Films," *J. Cryst. Growth*, **192** [3/4] 423 (1998).
8. H. Itoh, T. Uemura, H. Yamaguchi, and S. Naka, "Chemical Vapour Deposition of Epitaxial Ni-Zn Ferrite Films by Thermal Decomposition of Acetylacetonato Complexes," *J. Mater. Sci.*, **24** [10] 3549 (1989).
9. S. D. Sartale and C. D. Lokhande, "Electrochemical Synthesis of Nanocrystalline CoFe₂O₄ Thin Films and their Characterization," *Ceram. Int.*, **28** [5] 467-77 (2002).
10. V. Surve and V. Puri, "Some Properties of Electroless Plated Cobalt and Magnesium Ferrite Thin Films-Effect of pH and Time of Deposition," *Bull. Electrochem.*, **14** [4-5] 151 (1998).
11. S.-H. Yu, Yoshimura, and Masahiro, "Direct Fabrication of Ferrite MFe_2O_4 (M=Zn,Mg)/Fe Composite Thin Films by Soft Solution Processing," *Chem. Mater.*, **12** [12] 3805 (2000).

12. M. Taheri, E. E. Carpenter, V. Cestone, M. M. Miller, M. P. Raphael, M. E. McHenry, and V. G. Haris, "Magnetism and Structure of $Zn_xFe_{3-x}O_4$ Films Processed via Spin-Spray Deposition," *J. Appl. Phys.*, **91** [10] 7595 (2002).
13. N. Matsushita, C. P. Chong, T. Mizutani, and M. Abe, "Ni-Zn Ferrite Films with High Permeability ($\mu \sim 30$, $\mu \sim 30$) at 1 GHz Prepared at 90°C," *J. Appl. Phys.*, **91** [10] 7376 (2002).
14. J. G. dos S. Duque, M. A. Macedo, N. O. Moreno, J. L. Lopez, and H. D. Pfanos, "Magnetic and Structural Properties of $CoFe_2O_4$ Thin Films Synthesized via a Sol-Gel Process," *J. Magn. Magn. Mater.*, **226-230** 1424 (2001).
15. S. D. Sathaye, K. R. Patil, S. D. Kulkarni, P. P. Bakre, S. D. Pradhan, B. D. Sarwade, and S. N. Shintre, "Modification of Spin Coating Method and Its Application to Grow Thin Films of Cobalt Ferrite," *J. Mater. Sci.*, **38** [1] 29 (2003).
16. F. Cheng, Z. Peng, Z. C. Liao, and C. Yan, "The Sol-Gel Preparation and AFM Study of Spinel $CoFe_2O_4$ Thin Film," *Thin Solid Films*, **339** 109 (1999).
17. J. Ino, A. Hishinuma, H. Nagayama, and H. Kawahara, *Japanese Patent* 01093443A (Nippon Sheet Glass), June 7, (1988).
18. H. Nagayama, H. Honda, and H. Kawahara, "A New Process for Silica Coating," *J. Electrochem. Soc.*, **135** 2013 (1988).
19. S. Deki, Y. Aoi, O. Hiroi, and A. Kajinami, "Synthesis and Properties of Alkylthio-Substituted Tris-Fused Tetrathiafulvalenes," *Chem. Lett.*, 433 (1996).
20. S. Deki, Y. Aoi, Y. Miyake, A. Gotoh, and A. Kajinami, "Novel Wet Process for Preparation of Vanadium Oxide Thin Film," *Mater. Res. Bull.*, **31** [11] 1399 (1996).
21. K. Tsukuma, T. Akiyama, and H. Imai, "Liquid Phase Deposition Film of Tin Oxide," *J. Non-Cryst. Solids*, **210** 48 (1997).
22. P. Pramanik and S. Bhattacharya, "A Chemical Method for the Deposition of Nickel Oxide Thin Films," *J. Electrochem. Soc.*, **137** 3869 (1990).
23. M. Izaki and T. Omi, "Transparent Zinc Oxide Films Chemically Prepared from Aqueous Solution," *J. Electrochem. Soc.*, **144** L3 (1997).
24. H. Ko, Y. Yu, M. Mizuhata, A. Kajinami, and S. Deki, "Preparation of Au Nanoparticle Dispersed Nb_2O_5 Composite Film by Liquid Phase Deposition," *J. Electroan. Chem.*, **559** 91 (2003).
25. S. Deki, Y. Aoi, J. Okibe, H. Yanagimoto, A. Kajinami, and M. Mizuhata, "Preparation and Characterization of Iron Oxyhydroxide and Iron Oxide Thin Films by Liquid-Phase Deposition," *J. Mater. Chem.*, **7** 1769 (1997).
26. S. Deki, Y. Aoi, H. Yanagimoto, K. Ishii, K. Akamatsu, M. Mizuhata, and A. Kajinami, "Preparation and Characterization of Au-Dispersed TiO_2 Thin Films by a Liquid-Phase Deposition Method," *J. Mater. Chem.*, **6** 1879 (1996).
27. Y. Gao, Y. Masuda, T. Yinezawa, and K. Koumoto, "Site-Selective Deposition and Micropatterning of $SrTiO_3$ Thin Film on Self-Assembled Monolayers by the Liquid Phase Deposition Method," *Chem. Mater.*, **14** 5006 (2002).
28. S. Deki and Y. Aoi, "Synthesis of Metal Oxide Thin Films by Liquid-Phase Deposition Method," *J. Mater. Res.*, **13** [4] 883 (1998).
29. C. Dong, "PowderX: Windows-95-Based Program for Powder X-Ray Diffraction Data Processing," *J. Appl. Cryst.*, **32** 838 (1999).
30. W. Schiessi, W. Potzel, H. Kartzel, M. Steiner, G. Kalvius, A. Martin, M. Krause, I. Halevy, J. Gal, W. Schafer, G. Will, M. Hillberg, and R. Wappling, "Magnetic Properties of the $ZnFe_2O_4$ Spinel," *Phys. Rev. B*, **53** 9143 (1996).
31. H. P. Klug and L. E. Alexander, *X-Ray Diffraction Procedure for Polycrystalline and Amorphous Materials*; Wiley, New York, 2nd Ed., 1974.
32. K. Koumoto, S. Seo, T. Sugiyama, and W. S. Seo, "Micropatterning of Titanium Dioxide on Self-Assembled Monolayers Using a Liquid-Phase Deposition Process," *Chem. Mater.*, **11** (1999).
33. T. P. Niesen, J. Bill, and F. Aldinger, "Deposition of Titania Thin Films by a Peroxide Route on Different Functionalized Organic Self-Assembled Monolayers," *Chem. Mater.*, **13** 1552 (2001).
34. J. Smit and H. P. J. Wijn, *Ferrites*; Wiley, New York, 1959.
35. K. Tanaka, S. Nakashima, K. Fujita, and K. Hirao, "High Magnetization and the Faraday Effect for Ferrimagnetic Zinc Ferrite Thin Film," *J. Phys.: Condens. Matter*, **15** L469 (2003).